RAS Techniques and Instruments

RASTAI **2,** 33–44 (2023) https://doi.org/10.1093/rasti/rzac011
Advance Access publication 2023 January 14

Extending time-series models for irregular observational gaps with a moving average structure for astronomical sequences

C. Ojeda,[1] W. Palma,[2] S. Eyheramendy[2,3] and F. Elorrieta[2,4,5]★

[1]*Escuela de Estadística, Universidad del Valle, Cali 760042, Colombia*
[2]*Millennium Institute of Astrophysics, Santiago 7500011, Chile*
[3]*Faculty of Engineering and Sciences, Universidad Adolfo Ibañez, Diagonal Las Torres 2700, Peñalolén, Chile*
[4]*Departmento de Matemáticas, Facultad de Ciencia, Universidad de Santiago de Chile, Av. Libertador Bernardo O'Higgins 3663, Estacion Central, Santiago 9170022, Chile*
[5]*Center for Interdisciplinary Research in Astrophysics and Space Exploration (CIRAS), Universidad de Santiago de Chile, Av. Libertador Bernardo O'Higgins 3363, Estación Central, Chile*

Accepted 2022 December 9. Received 2022 October 5; in original form 2022 May 13

ABSTRACT

In this study, we introduce a novel moving-average model for analyzing stationary time-series observed irregularly in time. The process is strictly stationary and ergodic under normality and weakly stationary when normality is not assumed. Maximum likelihood (ML) estimation can be efficiently carried out through a Kalman algorithm obtained from the state-space representation of the model. The Kalman algorithm has order O(n) (where n is the number of observations in the sequence), from which it is possible to efficiently generate parameter estimators, linear predictors, and their mean-squared errors. Two procedures were developed for assessing parameter estimation errors: one based on the Hessian of the likelihood function and another one based on the bootstrap method. The behaviour of these estimators was assessed through Monte Carlo experiments. Both methods give accurate estimation performance, even with relatively small number of observations. Moreover, it is shown that for non-Gaussian data, specifically for the Student's t and generalized error distributions, the parameters of the model can be estimated precisely by ML. The proposed model is compared to the continuous autoregressive moving average (MA) models, showing better performance when the MA parameter is negative or close to one. We illustrate the implementation of the proposed model with light curves of variable stars from the OGLE and HIPPARCOS surveys and stochastic objects from Zwicky Transient Facility. The results suggest that the irregular MA model is a suitable alternative for modelling astronomical light curves, particularly when they have negative autocorrelation.

Key words: methods: data analysis – methods: statistical – galaxies: general.

1 INTRODUCTION

Time-series data observed at irregularly spaced intervals arise often in fields as diverse as astronomy, climatology, economics, finance, medical sciences, and geophysics (see, e.g. Moore, Visser & Shirtcliffe 1987; Muñoz et al. 1992; Belcher, Hampton & Tunnicliffe Wilson 1994; Corduas & Piccolo 2008; Hand 2008; Kim & Stoffer 2008; Harvill, Ravishanker & Ray 2013; Mudelsee 2014; Podgorski 2014; Babu & Mahabal 2016; Eyheramendy, Elorrieta & Palma 2018; Caceres et al. 2019; Edelmann, Fokianos & Pitsillou 2019; Elorrieta, Eyheramendy & Palma 2019; Miller 2019; Zhang 2020; Elorrieta et al. 2021). Although this type of data is very common in many areas, there are still not many methodologies with which to model them. Arguably because the statistical analysis of irregularly observed time-series poses several difficulties.

For example, it matters how the time-series data were obtained. Data can be regularly observed with missing observations, or the data can be truly irregularly observed with no underlying regular sampling interval. Moreover, a time-series may have both irregularly observed measurements and missing values. This may occur, for example, in astronomy where the measurement schedule may be irregularly in time and the scheduled observation cannot be made at the specified date due to climate conditions. There exist several methods to analyze time-series with missing values which are useful when we have data regularly observed but some of them are missing (see, e.g. Parzen 1963; Dunsmuir 1983; Reinsel & Wincek 1987). However, these methods can not be used when the data are truly irregularly observed. Mainly two approaches have been proposed for irregularly observed data. One such approach is based on interpolation, it transforms irregularly observed data into regularly observed so that conventional techniques can be applied (see, e.g. Adorf 1995). Another approach is when irregularly observed time-series can be treated as discrete realizations of a continuous stochastic process (see, e.g. Robinson 1977; Parzen 1984; Thornton & Chambers 2013).

Following the discrete-time approach, we have proposed autoregressive models for irregularly observed data, such as the irregularly observed autoregressive (iAR) (Eyheramendy et al. 2018), CiAR

★ E-mail: felipe.elorrieta@usach.cl

© The Author(s) 2023.
Published by Oxford University Press on behalf of Royal Astronomical Society. This is an Open Access article distributed under the terms of the Creative Commons Attribution License (http://creativecommons.org/licenses/by/4.0/), which permits unrestricted reuse, distribution, and reproduction in any medium, provided the original work is properly cited.

Downloaded from https://academic.oup.com/rasti/article/2/1/33/6987645 by guest on 22 January 2023

(Elorrieta et al. 2019), and the BiAR models (Elorrieta et al. 2021). Autoregressive processes impose a particular temporal correlation structure for a time-series sequence. A natural alternative serial dependency structure is the one encountered in MA models. In this paper, we described a novel MA model for irregularly observed sequences, the so-called irregular moving average (iMA) model. The iMA model allows the treatment of MA structures with irregularly observed times without assuming a continuous time or a regularly sampled underlying process. Apart from being able to fit irregularly spaced time-series data, the proposed model may be used for interpolating this type of time-series as well as forecasting future values.

Our model formulation allows to estimate both positive and negative serial correlations. This is an advantage with respect to the continuous autoregressive (CAR) model and the iAR model that can only estimate positive correlations. This can be an important issue with astronomical data. For example, Elorrieta et al. (2019) show that the harmonic processes commonly used to model light curves of variable stars have negative correlations for small periods.

The proposed iMA model is compared to the Continuous Autoregressive Moving Average (CARMA) models. Note that, a direct comparison is not possible. The CARMA (p, q) model, with autoregressive order p and MA order q, requires that $p > q$ to be stationary and have finite variance (see, Phadke & Wu 1974; Thornton & Chambers 2013). Consequently, the iMA process is not a particular case of the CARMA class of models. Nevertheless, in this paper, the iMA model is compared to the CARMA (2,1) processes. Observe that in the latter case, the model will have two additional parameters as compared to the iMA model. In these model comparisons, the iMA has, in general, better performance, as assessed in terms of log-likelihood, AIC and mean-squared error (MSE).

The remainder of the paper is organized as follows. In Section 2, we introduce a general class of ARMA processes for irregularly observed sequences, the so-called iARMA (Ojeda et al. 2022) and a novel class of stochastic processes for modelling irregularly spaced sequences with a MA (iMA) structure. Note that the iMA model is not a special case of the iARMA model. The iARMA model can only estimate positive autocorrelations whereas the iMA can estimate negative autocorrelations as well as positive. This section also provides a state-space representation of the model along with one-step linear predictors and their MSEs. The ML and bootstrap estimation methods are introduced in Section 3.1. The finite-sample behaviours of the proposed estimators are studied via Monte Carlo in Section 4, for Gaussian and non-Gaussian error distributions. Two real-life data applications are discussed in Section 5 while conclusions are presented in Section 6. Finally, some technical results are provided in the appendix section.

2 THE MODELS

In this section, we present the iARMA and the iMA discrete-time irregularly observed models. It is assumed that all joint moments up to order two are finite and that the pattern of irregular spacing is independent of the stochastic process properties. Further, let $\mathbb{T} = \{t_n\}_{n\in\mathbb{N}^+}$ be a set of given times so that its consecutive differences, $\Delta_{n+1} = t_{n+1} - t_n$, are such that there is $\Delta_L > 0$ and $\Delta_L \leq \Delta_{n+1}$ for all n. Without loss of generality, it is assumed that $\Delta_L = 1$. Otherwise, each t_n can be rescaled by Δ_L. Note that these conditions are compatible with any physical measurement and determine $\mathbb{T}$ as a discrete subset of $\mathbb{R}$.

2.1 The iARMA model

The iARMA model (Ojeda et al. 2022), is a stationary stochastic process with an autoregressive MA structure that allows irregularly observational times. The iARMA model is defined in the following way.

Let $\{\varepsilon_{t_n}\}_{t_n\in\mathbb{T}}$ be a sequence of uncorrelated random variables with mean 0 and variance $\sigma^2 c_n(\phi, \theta)$ where $\sigma^2 > 0$, $0 \leq \phi, \theta < 1$, $c_1(\phi, \theta) = \frac{1+2\theta\phi+\theta^2}{1-\phi^2}$, and

$$c_{n+1}(\phi, \theta) = c_1(\phi, \theta)(1 - \phi^{2\Delta_{n+1}}) - 2\phi^{\Delta_{n+1}}\theta^{\Delta_{n+1}} - \frac{\theta^{2\Delta_{n+1}}}{c_n(\phi, \theta)}.$$

The iARMA model in its state-space representation is defined as the process $\{X_{t_n}\}$ such that

$$X_{t_n} = \alpha_{t_n} + \varepsilon_{t_n},\ \alpha_{t_1} = 0,$$
$$\alpha_{t_{n+1}} = \phi^{\Delta_{n+1}}\alpha_{t_n} + \left(\phi^{\Delta_{n+1}} + \frac{\theta^{\Delta_{n+1}}}{c_n(\phi, \theta)}\right)\varepsilon_{t_n}.$$

In this model, when $\theta = 0$, the so-called iAR process (Eyheramendy et al. 2018) is obtained, while when $\phi = 0$ the process corresponds to the iMA, which is described in the following section.

The mean and the autocovariance functions of the iARMA model are given by

$$\mathrm{E}(X_{t_n}) = 0, \quad \text{and}$$
$$\mathrm{Cov}(X_{t_n}, X_{t_{n+k}}) = \begin{cases} \sigma^2 c_1(\phi, \theta), & k = 0, \\ \gamma_{n+1}(\phi, \theta), & k = 1, \\ \phi^{t_{n+k}-t_{n+1}}\gamma_{n+1}(\phi, \theta), & k \geq 2, \end{cases}$$

for all n, where $\gamma_{n+1}(\phi, \theta) = \sigma^2[\phi^{\Delta_{n+1}} c_1(\phi, \theta) + \theta^{\Delta_{n+1}}]$. The autocorrelation function is given by

$$\mathrm{Cor}(X_{t_n}, X_{t_{n+k}}) = \begin{cases} 1, & k = 0, \\ \rho_{n+1}(\phi, \theta), & k = 1, \\ \phi^{t_{n+k}-t_{n+1}}\rho_{n+1}(\phi, \theta), & k \geq 2, \end{cases}$$

for all n, where $\rho_{n+1}(\phi, \theta) = \phi^{\Delta_{n+1}} + \theta^{\Delta_{n+1}}/c_1(\phi, \theta)$.

A drawback of this model is that its autocorrelation function is defined only for positive values. In the next section, we present the iMA model that allows negative correlations with a MA structure. This methodology offers an alternative approach to the CiAR model when handling negative serial correlation.

2.2 Irregular moving average model

DEFINITION 1 (THE IMA MODEL). Let $\{\varepsilon_{t_n}\}_{t_n\in\mathbb{T}}$ be a sequence of uncorrelated random variables with mean 0, and variance $\sigma^2 c_n(\theta)$, where $\sigma^2 > 0$, $|\theta| < 1$, $c_1(\theta) = 1 + \theta^2$, and

$$c_{n+1}(\theta) = c_1(\theta) - \frac{\gamma_{n+1}(\theta)^2}{c_n(\theta)},$$

with $\gamma_{n+1}(\theta) = \mathrm{sign}(\theta)|\theta|^{\Delta_{n+1}}$. The process $\{X_{t_n}\}_{t_n\in\mathbb{T}}$, is said to be an iMA process if $X_{t_1} = \varepsilon_{t_1}$, and

$$X_{t_{n+1}} = \varepsilon_{t_{n+1}} + \frac{\gamma_{n+1}(\theta)}{c_n(\theta)}\varepsilon_{t_n}. \tag{1}$$

It is said that $\{X_{t_n}\}_{t_n\in\mathbb{T}}$ is an iMA process with mean μ if $\{X_{t_n} - \mu\}_{t_n\in\mathbb{T}}$ is an iMA process.

Downloaded from https://academic.oup.com/rasti/article/2/1/33/6987645 by guest on 22 January 2023

2.3 Properties

For the iMA process, the mean and the autocovariance functions are given by

$$\mathrm{E}(X_{t_n}) = 0, \quad \text{and} \quad \mathrm{Cov}(X_{t_n}, X_{t_{n+k}}) = \begin{cases} \sigma^2 c_1(\theta), & k = 0, \\ \sigma^2 \gamma_{n+1}(\theta), & k = 1, \\ 0, & k \geq 2, \end{cases}$$

for all n. The autocorrelation function is

$$\mathrm{Cor}(X_{t_n}, X_{t_{n+k}}) = \begin{cases} 1, & k = 0, \\ \gamma_{n+1}(\theta)/c_1(\theta), & k = 1, \\ 0, & k \geq 2, \end{cases}$$

for all n. Since it has a constant mean and its covariance function depends only on the time differences, the process is weakly stationary. Further, if $\{\varepsilon_{t_n}\}_{t_n \in \mathbb{T}}$ is an i.i.d. sequence and $\mathrm{E}|\varepsilon_{t_n}|^r < \infty$ for some $r > 2$, the iMA process is second-moment ergodic (Hamilton 1994, pp. 47). In particular, under Gaussianity in the errors, the process is strictly stationary and ergodic for all moments (Stout 1974, Theorem 3.5.8, pp. 182). Ergodicity refers to the property of a stationary stochastic process, which will enable to use a single sequence in order to estimate reliably the moments of the distribution underlying the stochastic process (Spanos 1999).

Another property of the iMA model is that it is a more general process since when $\Delta_{n+1} = 1$, for all n, the traditional first-order MA model is obtained. It is relevant to notice that an MA (1) process with missing values is not equivalent to an iMA model. Given the serial dependence of the MA (1) process, a missing value generates two independent blocks of data. On the contrary, an iMA model that is observed skipping one time period still possesses serial dependence. A practical consequence of this distinction is that an iMA model cannot be simulated by generating missing values in a MA (1) process. This aspect can be formally expressed in the following result which has a direct proof.

LEMMA 1. *Let* $\{\mathrm{y}_1, \mathrm{y}_2, \ldots, \mathrm{y}_n, \mathrm{y}_{n+1}, \ldots, \mathrm{y}_N\}$ *be a sequence from a Gaussian MA(1) process, where* $y_t = \varepsilon_t + \theta\, \varepsilon_{t-1}$ *and* $\{\varepsilon_t\}$ *are Gaussian independent random variables. If the value* y_n*, with* $1 < \mathrm{n} < \mathrm{N}$*, is missing at random, then the blocks* $\{\mathrm{y}_1, \mathrm{y}_2, \ldots, \mathrm{y}_{n-1}\}$ *and* $\{\mathrm{y}_{n+1}, \ldots, \mathrm{y}_N\}$ *are independent.*

Proof. Let B_1 be the first block of observations $\{y_1, y_2, \ldots, y_{n-1}\}$ and B_2 be the second block $\{y_{n+1}, \ldots, y_N\}$. Given that $y_t = \varepsilon_t + \theta\, \varepsilon_{t-1}$, we may write $B_1 = B_1(\varepsilon_0, \ldots, \varepsilon_{n-1})$ and $B_2 = B_2(\varepsilon_n, \ldots, \varepsilon_N)$. Since the sequences $\{\varepsilon_0, \ldots, \varepsilon_{n-1}\}$ and $\{\varepsilon_n, \ldots, \varepsilon_N\}$ are independent, we conclude that the blocks B_1 and B_2 are independent as well. □

2.4 State-space representation

From Definition 1, a state-space representation of the model (1) can be obtained. This representation has the lowest dimension of the state vector and is given by

$$X_{t_n} = \alpha_{t_n} + \varepsilon_{t_n}, \quad \alpha_{t_1} = 0, \quad \alpha_{t_{n+1}} = \frac{\gamma_{n+1}(\theta)}{c_n(\theta)} \varepsilon_{t_n},$$

In this representation, the transition and measurement equation disturbances are correlated. As is suggested by Harvey (1989), to get a new system on which these disturbances are uncorrelated, the following expressions can be used,

$$X_{t_n} = \alpha_{t_n} + \varepsilon_{t_n}, \quad \alpha_{t_1} = 0, \quad \alpha_{t_{n+1}} = \frac{\gamma_{n+1}(\theta)}{c_n(\theta)} X_{t_n} - \frac{\gamma_{n+1}(\theta)}{c_n(\theta)} \alpha_{t_n}. \quad (2)$$

The inclusion of X_{t_n} in (2) does not affect the Kalman filter, as X_{t_n} is known at time t_n.

2.5 Prediction

Using the innovations algorithm from Brockwell & Davis (1991), the one-step linear predictors are $\hat{X}_{t_1}(\theta) = 0$, with MSE $\mathrm{E}[(X_{t_1} - \hat{X}_{t_1}(\theta))^2] = \sigma^2 c_1(\theta)$, and

$$\hat{X}_{t_{n+1}}(\theta) = \frac{\gamma_{n+1}(\theta)}{c_n(\theta)} (X_{t_n} - \hat{X}_{t_n}(\theta)),$$

with MSEs $\mathrm{E}[(X_{t_{n+11}} - \hat{X}_{t_{n+1}}(\theta))^2] = \sigma^2 c_{n+1}(\theta)$. Note that these equations also can be obtained through the Kalman filter.

3 ESTIMATION

3.1 Maximum likelihood method

Let X_t be observed at points $t_1, \ldots, t_{\mathrm{N}}$. The log-likelihood under Gaussianity in the errors is

$$-\frac{N}{2} \ln 2\pi - \frac{N}{2} \ln \sigma^2 - \frac{1}{2} \sum_{n=1}^{N} \ln c_n(\theta) - \frac{1}{2} \sum_{n=1}^{N} \frac{(X_{t_n} - \hat{X}_{t_n}(\theta))^2}{\sigma^2 c_n(\theta)},$$

where θ and σ^2 are any admissible parameter values. Now, optimizing it for σ^2, replacing the optimum value into the log-likelihood, and organizing terms, the reduced likelihood is obtained (Brockwell & Davis 1991)

$$q_N(\theta) = \ln \hat{\sigma}_N^2(\theta) + \frac{1}{N} \sum_{n=1}^{N} \ln c_n(\theta), \quad (3)$$

where

$$\hat{\sigma}_{\mathrm{N}}^2(\theta) = \frac{1}{\mathrm{N}} \sum_{n=1}^{\mathrm{N}} \frac{(X_{t_n} - \hat{X}_{t_n}(\theta))^2}{c_n(\theta)}.$$

The maximum likelihood (ML) estimate of θ, $\hat{\theta}_N$, is the value minimizing $q_{\mathrm{N}}(\theta)$. The estimate of σ^2 is $\hat{\sigma}_N^2 = \hat{\sigma}_N^2(\hat{\theta}_N)$. The optimization process can be done through the method proposed by Byrd et al. (1995), which allows general box constraints. In other words, $q_{\mathrm{N}}(\theta)$ can be minimized under the constraint $-1 < \theta < 1$. Also, this method allows for finding the numerically differentiated Hessian matrix at $\hat{\theta}_N$. Solving it, the estimated standard error, $\hat{\mathrm{se}}(\hat{\theta}_N)$, can be obtained (see, e.g, Hamilton 1994, Section 5.8, pp. 142). Based on the ML estimator properties, we can test the significance of the estimate of the parameter θ with a Wald test of size α through the p-value defined as $P(|Z| > |Z_0|)$ where $Z_0 = \hat{\theta}_N / \hat{\mathrm{se}}(\hat{\theta}_N)$.

3.2 Bootstrap method

In order to carry out statistical inference, it is necessary to derive the distribution of the statistics used for the estimation of the parameters from the data, but these calculations are often cumbersome. Additionally, if N is small, or if the parameters are close to the boundary 1 where the invertibility property cannot be achieved, the asymptotic approximations can be quite poor (Shumway & Stoffer 2017). Further, in the irregularly observed time case, the asymptotic approximations need to establish strong conditions (Robinson 1977, Section 4, pp.12), which are difficult to attain. To overcome these difficulties and to get approximations of the finite sample distributions, the bootstrap method can be used.

Downloaded from https://academic.oup.com/rasti/article/2/1/33/6987645 by guest on 22 January 2023

The usual procedure for applying the bootstrap method in time-series consists of fitting a suitable model to the data to obtain the residuals from the fitted model and then generate a new series by incorporating random samples from the residuals into the fitted model. The residuals are typically centred to have the same mean as the innovations of the model.

Specifically, to apply the bootstrap method to the estimation of θ in the iMA model (assuming $\sigma^2 = 1$), let X_t be observed at points $t_1, \ldots, t_N$, and consider $\hat{\theta}_N$ as the ML estimator. The standardized estimated innovations are

$$e^s_{t_n} = \frac{X_{t_n} - \hat{X}_{t_n}(\hat{\theta}_N)}{\sqrt{c_n(\hat{\theta}_N)}}.$$

The so-called model-based resampling might proceed by equi-probable sampling with replacement from centred residuals $e^{sc}_{t_1} = e^s_{t_1} - \bar{e}, \ldots, e^{sc}_{t_N} = e^s_{t_N} - \bar{e}$, where $\bar{e} = \sum_{n=1}^{N} e^s_{t_n}/N$, to obtain simulated innovations $e^{sc}_{t_1^*}, \ldots, e^{sc}_{t_N^*}$, with $t_1^*, \ldots, t_N^*$ the sampled times, which in our experiments are considered to be the same as the observational times, and then defining

$$X^*_{t_1} = \sqrt{c_1(\hat{\theta}_N)}e^{sc}_{t_1^*},$$
$$X^*_{t_{n+1}} = \sqrt{c_{n+1}(\hat{\theta}_N)}e^{sc}_{t^*_{n+1}} + \frac{\gamma_{n+1}(\hat{\theta}_N)}{c_n(\hat{\theta}_N)}\sqrt{c_n(\hat{\theta}_N)}e^{sc}_{t_n^*}.$$

as the bootstrapped sequence. Thus, the parameters can be estimated via ML assuming that the data are $X^*_{t_n}$ for $n = 1, \ldots, N$. This process is repeated B times, generating a collection of bootstrapped parameter estimates. Finally, the finite sample distribution of the estimator, $\hat{\theta}_N$, is estimated from the bootstrapped parameter values. The bootstrap estimate is the mean of this sample distribution, and the standard deviation is the estimated standard error. Appendix A shows that resampling is proper for the iMA model.

4 SIMULATIONS

This section provides a Monte Carlo study that assesses the finite-sample performance of the ML and bootstrap estimators. In this study, M = 1000 series or trajectories of size N, i.e. $x_{t_1}, \ldots, x_{t_N}$ are simulated from the IMA model (1) for different values of θ and N. The simulation consider,

$$\theta \in \{-0.9, -0.7, -0.5, 0.5, 0.7, 0.9\}, \text{ and } N \in \{300, 1000\}.$$

For each simulated series, the parameter θ is estimated through the ML and bootstrap methods described in Sections 3.1 and 3.2, respectively. It is established as regular ($\Delta_n = 1$ for $n = 2, \ldots, N$) as well as irregular spaced times, $t_1, \ldots, t_N$, where

$$\Delta_n \overset{\text{ind}}{\sim} 1 + \exp(\lambda = 1), \quad \text{for } n = 2, \ldots, N.$$

4.1 ML estimator

Let $\hat{\theta}^{\text{MLE}}_m$ be the ML estimation obtained by minimizing (3) and $\widehat{\text{se}}(\hat{\theta}^{\text{MLE}}_m)$ be the estimated standard error for the mth simulated series. The standard error is estimated through the curvature of the likelihood surface at $\hat{\theta}^{\text{MLE}}_m$ (see, section 3.1). As a summary of the estimator's performance is used the mean value of the M ML estimates and their respective estimated standard errors as follow:

$$\hat{\theta}^{\text{MLE}} = \frac{1}{M}\sum_{m=1}^{M}\hat{\theta}^{\text{MLE}}_m \quad \text{and} \quad \widehat{se}(\hat{\theta}^{\text{MLE}}) = \frac{1}{M}\sum_{m=1}^{M}\widehat{se}\left(\hat{\theta}^{\text{MLE}}_m\right).$$

4.2 Bootstrap estimator

For each simulated series, $B = 500$ bootstrap series are sampled from which a bootstrap estimator is obtained by minimizing (3). Let $\hat{\theta}^{\text{b}}_{m,j}$ be the jth bootstrap estimation for the mth simulated series with $j = 1, \ldots, B$ and $m = 1, \ldots, M$. The bootstrap estimation and the estimated variance error for a simulated series are defined as

$$\hat{\theta}^b_m = \frac{1}{B}\sum_{j=1}^{B}\hat{\theta}^b_{m,j} \quad \text{and} \quad \widehat{\text{se}}^2\left(\hat{\theta}^b_m\right) = \frac{1}{B-1}\sum_{j=1}^{B}\left(\hat{\theta}^b_{m,j} - \hat{\theta}^b_m\right)^2,$$

Finally, the performance evaluation is done through the mean value of the M bootstrap estimations and their respective estimated standard errors as follow:

$$\hat{\theta}^{\text{b}} = \frac{1}{\text{M}}\sum_{m=1}^{\text{M}}\hat{\theta}^{\text{b}}_m \quad \text{and} \quad \widehat{\text{se}}(\hat{\theta}^{\text{b}}) = \frac{1}{\text{M}}\sum_{m=1}^{\text{M}}\widehat{\text{se}}\left(\hat{\theta}^{\text{b}}_m\right).$$

4.3 Performance measures

As a measure of the estimator performance, the root mean square error (RMSE) and the coefficient of variation (CV) are considered. These are defined as

$$\text{RMSE}_{\hat{\theta}^{\text{MLE}}} = \left(\widehat{\text{se}}(\hat{\theta}^{\text{MLE}})^2 + \text{bias}^2_{\hat{\theta}^{\text{MLE}}}\right)^{1/2}, \text{ and}$$
$$\text{CV}_{\hat{\theta}^{\text{MLE}}} = \frac{\widehat{\text{se}}(\hat{\theta}^{\text{MLE}})}{\left|\hat{\theta}^{\text{MLE}}\right|},$$

where $\text{bias}_{\hat{\theta}^{\text{MLE}}} = E(\hat{\theta}^{\text{MLE}}) - \theta$. Also, an approximate variance estimator is given by

$$\widetilde{\text{se}}^2(\hat{\theta}^{\text{MLE}}) = \frac{1}{M-1}\sum_{m=1}^{M}\left(\hat{\theta}^{\text{MLE}}_m - \hat{\theta}^{\text{MLE}}\right)^2.$$

$\text{RMSE}_{\hat{\theta}^{\text{b}}}$, $\text{CV}_{\hat{\theta}^{\text{b}}}$, $\text{bias}_{\hat{\theta}^{\text{b}}}$, and $\widetilde{\text{se}}^2(\hat{\theta}^{\text{b}})$ can be defined analogously.

Finally, the Monte Carlo error (MCE) is estimated for every simulation via asymptotic theory (see, Koehler, Brown & Haneuse 2009) through

$$\frac{\widetilde{\text{se}}(\hat{\theta}^{\text{MLE}})}{\sqrt{M}}.$$

The MCE is a estimation of the standard deviation of the Monte Carlo estimator, taken across repetitions of the simulation, where each simulation is based on the same design and consists of M replications.

4.4 Finite sample distributions for ML and bootstrap estimators

As an estimation of the finite sample distributions for ML and bootstrap estimators, Fig. 1 shows the densities calculated from the 1000 estimates obtained from the simulations configured by different values of θ and N. In general, these show symmetry and bell-shaped forms. Also, they seem to be unbiased since the mean of the estimated values are close to their theoretical values. However, for small values of θ, the estimates have greater variability. This behaviour is similar to that obtained when the traditional MA model is assumed since, in this case, the standard error of the ML estimator increases when the MA parameter decreases (see equation B1).

Tables 1 and 2 show the performance measures of the estimators, for the ML and bootstrap methods, respectively. Bias and variance are smaller when N increases as expected. Both methods provide good estimations for the standard error. Note that, these results

Downloaded from https://academic.oup.com/rasti/article/2/1/33/6987645 by guest on 22 January 2023

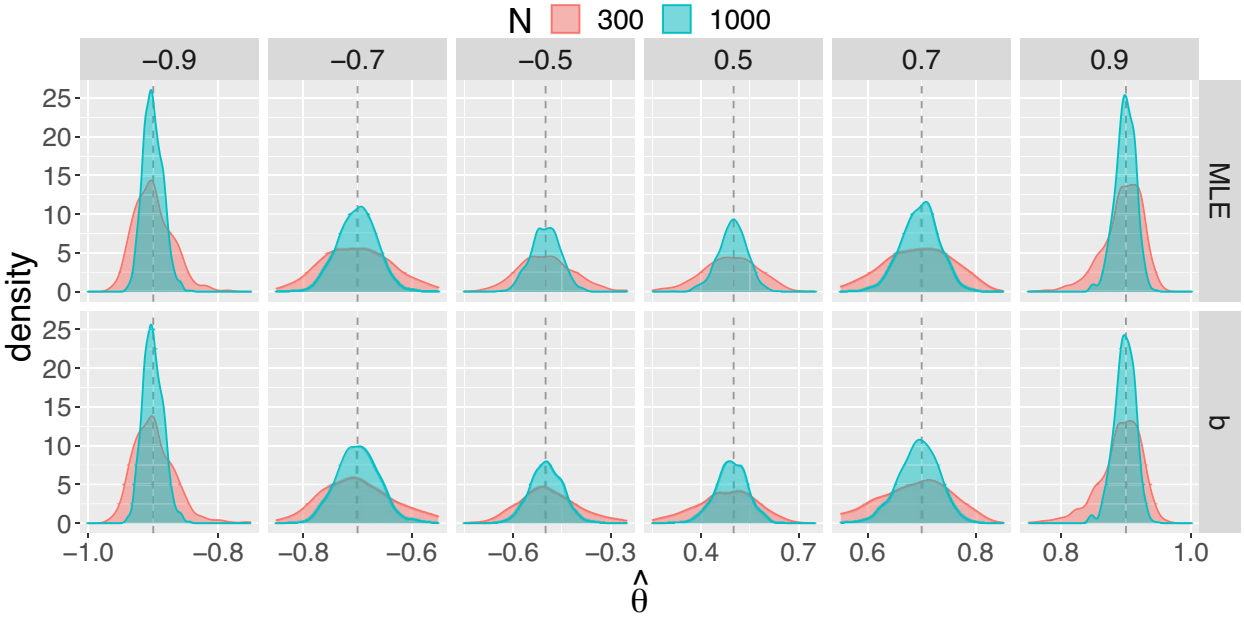


Figure 1. Densities were calculated for both the ML estimator (on the top panel) and the bootstrap estimator (on the bottom panel) from the 1000 estimates obtained from the simulations configured by different values of θ and sample sizes N. The dashed line corresponds to the theoretical values to be estimated.

Table 1. Monte Carlo results for the ML estimator with irregularly spaced times. The maximum MCE estimated (across scenarios) is 0.0005.

N	θ	$\hat{\theta}^{\text{MLE}}$	$\widehat{\text{se}}(\hat{\theta}^{\text{MLE}})$	$\widetilde{\text{se}}(\hat{\theta}^{\text{MLE}})$	$\text{bias}_{\hat{\theta}\text{MLE}}$	$\text{RMSE}_{\hat{\theta}\text{MLE}}$	$\text{CV}_{\hat{\theta}\text{MLE}}$
300	−0.9	−0.90	0.03	0.04	0.00	0.03	0.03
	−0.7	−0.70	0.06	0.07	0.00	0.06	0.09
	−0.5	−0.50	0.08	0.08	0.00	0.08	0.16
	0.5	0.49	0.08	0.09	−0.01	0.08	0.17
	0.7	0.69	0.06	0.07	−0.01	0.06	0.09
	0.9	0.90	0.03	0.03	−0.00	0.03	0.03
1000	−0.9	−0.90	0.02	0.02	−0.00	0.02	0.02
	−0.7	−0.70	0.04	0.04	−0.00	0.04	0.05
	−0.5	−0.50	0.04	0.04	−0.00	0.04	0.09
	0.5	0.50	0.04	0.04	−0.00	0.04	0.09
	0.7	0.70	0.04	0.04	−0.00	0.04	0.05
	0.9	0.90	0.02	0.02	−0.00	0.02	0.02

Table 2. Monte Carlo results for the bootstrap estimator with irregularly spaced times. The maximum MCE estimated (across scenarios) is 0.0005.

N	θ	$\hat{\theta}^{\text{b}}$	$\widehat{\text{se}}(\hat{\theta}^{\text{b}})$	$\widetilde{\text{se}}(\hat{\theta}^{\text{b}})$	$\text{bias}_{\hat{\theta}\text{b}}$	$\text{RMSE}_{\hat{\theta}\text{b}}$	$\text{CV}_{\hat{\theta}\text{b}}$
300	−0.9	−0.90	0.03	0.05	0.00	0.03	0.04
	−0.7	−0.69	0.07	0.07	0.01	0.07	0.10
	−0.5	−0.49	0.09	0.10	0.01	0.09	0.18
	0.5	0.47	0.09	0.10	−0.03	0.10	0.19
	0.7	0.68	0.07	0.07	−0.02	0.07	0.10
	0.9	0.89	0.03	0.03	−0.01	0.03	0.04
1000	−0.9	−0.90	0.02	0.02	−0.00	0.02	0.02
	−0.7	−0.70	0.04	0.04	0.00	0.04	0.05
	−0.5	−0.50	0.04	0.05	0.00	0.05	0.09
	0.5	0.49	0.05	0.05	−0.01	0.05	0.09
	0.7	0.69	0.04	0.04	−0.01	0.04	0.05
	0.9	0.90	0.02	0.02	−0.00	0.02	0.02

are consistent for both negative and positive values of θ. Also, the irregularly spaced times seem to increase the estimation variability. In Appendix B, the case with regular obsevational times is presented. In this case, the iMA model is reduced to the conventional MA model, and the results are equally consistent.

A second simulation experiment is performed in order to assess the performance of the CARMA (p, q) model in fitting an iMA simulated process. The CARMA models have been generally used to fit irregularly sampled time-series. However, as mentioned previously, the CARMA models are restricted to $p > q$, so the iMA model is not a particular case of the CARMA model (see, Phadke & Wu 1974; Thornton & Chambers 2013). For this reason, it is interesting to evaluate whether a CARMA model can properly fit an iMA process.

In this experiment, we generate 1000 sequences of the iMA process with two different lengths and four different values of the θ parameter. The irregular times were generated using a mixture of two exponential distributions with 130 and 6.5 as the means of the exponential distributions and 0.15 and 0.85 as their respective weights. We chose this distribution of times in order to obtain large time gaps, which can be an issue when a model assumes continuous time.

In order to fit the CARMA model, we use the function *carma* of the *growth* package in *R*. Because we are comparing with the iMA model, which has just one parameter, the closest CARMA model with which the iMA can be compared is the CARMA (2,1). Further, the root mean squared error was used as the goodness-of-fit measure. Table 3 presents the Monte Carlo results of this experiment. Note that the iMA model consistently outperforms the CARMA (2,1) model. In particular, for large values of θ and N the iMA model have almost 100 per cent of success rate when selecting the model with lowest RMSE. Furthermore, the success rate is even higher when the values of θ are negative. In Appendix C, we consider other goodness-of-fit measures such as the Akaike Criterion and the –2 log-likelihood. Considering these criteria, the iMA model also fits the simulated processes better than the CARMA (2,1) model in most cases. This result is relevant because when using the –2 log likelihood as a goodness-of-fit measure we are not penalizing by the number of parameters and still the iMA model has better performance than the CARMA model.

Downloaded from https://academic.oup.com/rasti/article/2/1/33/6987645 by guest on 22 January 2023

Table 3. Monte Carlo results of the experiment to compare the performance of the iMA and CARMA (2,1) models in fitting iMA model. The goodness of fit measure estimated from both models is the root mean squared error.

N	θ	$\hat{\theta}$	$\widehat{se}(\hat{\theta})$	RMSE_iMA	SD (RMSE_iMA)	RMSE_C21	SD (RMSE_C21)	% success
300	−0.9	−0.9029	0.0270	1.1331	0.0461	1.2908	0.0807	100.00
	−0.7	−0.7048	0.0569	1.1211	0.0455	1.2012	0.0572	99.30
	−0.5	−0.5029	0.0715	1.0746	0.0435	1.1007	0.0474	95.70
	0.5	0.4910	0.0715	1.0747	0.0435	1.0786	0.0453	60.50
	0.7	0.6932	0.0576	1.1212	0.0454	1.1298	0.0476	80.20
	0.9	0.8973	0.0283	1.1330	0.0458	1.1854	0.0525	99.70
1000	−0.9	−0.9009	0.0149	1.1349	0.0252	1.3212	0.0524	100.00
	−0.7	−0.7018	0.0311	1.1233	0.0249	1.2111	0.0328	100.00
	−0.5	−0.5019	0.0387	1.0765	0.0237	1.1089	0.0262	99.40
	0.5	0.4974	0.0387	1.0765	0.0238	1.0838	0.0258	76.30
	0.7	0.6981	0.0312	1.1233	0.0249	1.1340	0.0256	98.60
	0.9	0.8992	0.0151	1.1349	0.0252	1.1904	0.0283	100.00

Table 4. Monte Carlo results for the QML estimator with irregularly spaced times and Student's t errors with shape parameter $\nu = 7$. The maximum MCE estimated (across scenarios) is 0.0005.

N	θ	$\hat{\theta}^{MLE}$	$\widehat{se}(\hat{\theta}^{MLE})$	$\widetilde{se}(\hat{\theta}^{MLE})$	$bias_{\hat{\theta}MLE}$	$RMSE_{\hat{\theta}MLE}$	$CV_{\hat{\theta}MLE}$
300	−0.9	−0.90	0.03	0.03	−0.00	0.03	0.03
	−0.7	−0.70	0.06	0.06	−0.00	0.06	0.08
	−0.5	−0.50	0.07	0.08	0.00	0.07	0.14
	0.5	0.49	0.07	0.08	−0.01	0.07	0.15
	0.7	0.70	0.06	0.06	−0.00	0.06	0.08
	0.9	0.90	0.03	0.03	−0.00	0.03	0.03
1000	−0.9	−0.90	0.01	0.02	−0.00	0.01	0.02
	−0.7	−0.70	0.03	0.03	−0.00	0.03	0.04
	−0.5	−0.50	0.04	0.04	−0.00	0.04	0.08
	0.5	0.50	0.04	0.04	−0.00	0.04	0.08
	0.7	0.70	0.03	0.03	−0.00	0.03	0.04
	0.9	0.90	0.02	0.02	−0.00	0.02	0.02

Table 5. Monte Carlo results for the QML estimator with irregularly spaced times and generalized errors with shape parameter $\kappa = 1.28$. The maximum MCE estimated (across scenarios) is 0.0005.

N	θ	$\hat{\theta}^{MLE}$	$\widehat{se}(\hat{\theta}^{MLE})$	$\widetilde{se}(\hat{\theta}^{MLE})$	$bias_{\hat{\theta}MLE}$	$RMSE_{\hat{\theta}MLE}$	$CV_{\hat{\theta}MLE}$
300	−0.9	−0.90	0.03	0.03	−0.00	0.03	0.03
	−0.7	−0.70	0.06	0.06	0.00	0.06	0.08
	−0.5	−0.50	0.07	0.07	0.00	0.07	0.14
	0.5	0.49	0.07	0.08	−0.01	0.07	0.15
	0.7	0.69	0.06	0.06	−0.01	0.06	0.08
	0.9	0.90	0.03	0.03	−0.00	0.03	0.03
1000	−0.9	−0.90	0.01	0.02	−0.00	0.01	0.02
	−0.7	−0.70	0.03	0.03	−0.00	0.03	0.04
	−0.5	−0.50	0.04	0.04	0.00	0.04	0.08
	0.5	0.50	0.04	0.04	−0.00	0.04	0.08
	0.7	0.70	0.03	0.03	−0.00	0.03	0.04
	0.9	0.90	0.01	0.02	0.00	0.01	0.02

4.5 Non-Gaussian errors

There are many applications where Gaussian assumption is misspecified, but it is assumed in the likelihood to obtain the ML estimator. This estimator is commonly known as quasi-ML estimator or QMLE.

This section shows the performance measures for the QMLE in a Monte Carlo experiment where simulated sequences of the iMA model with non-Gaussian errors are generated. First, it is used a Student's t distribution with shape parameter ν (degree of freedom) defined as

$$f(z \mid \nu) = \frac{\Gamma\left(\frac{\nu+1}{2}\right)}{\sqrt{(\nu-2)\pi}\,\Gamma\left(\frac{\nu}{2}\right)}\left(1+\frac{z^2}{(\nu-2)}\right)^{-\left(\frac{\nu+1}{2}\right)}, \quad \nu > 2.$$

Second, a generalized error distribution with shape parameter κ defined as

$$f(z \mid \kappa) = \frac{\kappa e^{-0.5\left|\left(\sqrt{2^{-2/\kappa}\frac{\Gamma(\kappa^{-1})}{\Gamma(3\kappa^{-1})}}\right)^{-1} z\right|^{\kappa}}}{\sqrt{2^{-2/\kappa}\frac{\Gamma(\kappa^{-1})}{\Gamma(3\kappa^{-1})}}\,2^{1+\kappa^{-1}}\Gamma\left(\kappa^{-1}\right)}, \quad \kappa > 0,$$

is used. Both distributions are standardized according to specifications used by Ghalanos (2020).

Tables 4 and 5 display the results obtained for Student's t with $\nu = 7$ and generalized errors with $\kappa = 1.28$ (heavy tails), respectively. In both cases, the performance obtained for the QMLE is very similar to the performance obtained for the MLE presented in Table 1 (Gaussian case). This suggests that the QML estimator is robust to deviations from Gaussianity. Tables D1 and D2 in Appendix D show the performance obtained when non-Gaussian errors are assumed for the bootstrap estimator. Like the QMLE, the bootstrap estimator is robust to deviations from Gaussianity.

5 APPLICATIONS

We present the implementation of the models in two data sets from the following astronomical surveys: OGLE (Udalski et al. 1999), Hipparcos (Perryman et al. 1997) and the Zwicky Transient Facility (ZTF) (Bellm et al. 2018). In this application, we propose a two-step procedure. In the first step, it is aimed to determine if the iARMA model is an *appropriate and sufficient model* to explain the time dependency of the light curve. We define that the iARMA is an *appropriate and sufficient model* if either one or both of the parameters of the model are significant. In the second step, among the light curves that found an appropiate iARMA model, it is verified through the significance of the estimated parameters whether the model can be reduced to an iAR, iMA, or a white noise process. Note that the iAR model is a special case of an iARMA model and, for positive autocorrelation, the iMA model is a special case of an iARMA model as well. But the iMA also allows for negative autocorrelation, whereas the iARMA is restricted to the estimation of positive autocorrelation. Therefore, we are interested in assessing whether the autocorrelation of the light curve is positive or negative. With this application, we aim to show that the iMA model proposed in this work offers an alternative for fitting some light curves, particularly in the cases of negative autocorrelation.

Downloaded from https://academic.oup.com/rasti/article/2/1/33/6987645 by guest on 22 January 2023

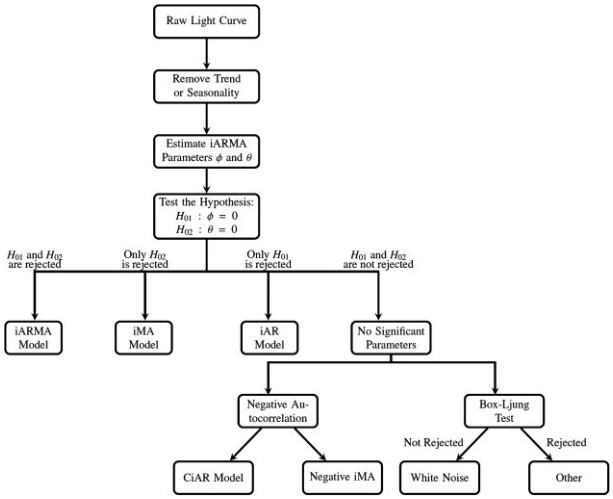


Figure 2. Flowchart of the selection procedure for discrete-time irregularly observed models used in the real-data applications.

The flowchart of the model selection procedure used in the following applications is shown in Fig. 2.

5.1 iARMA model fitting in the OGLE and Hipparcos light-curves data

We fit the iARMA model in 1171 periodic variable star light curves observed in the OGLE and HIPPARCOS survey. In order to fulfill the assumption that the time gaps need to be greater than one, same-day observations are represented by their mean and rescaled. Consequently, the observational times are defined as $\bar{t}_n$. Later, we rescaled $\bar{t}_n$ by the expression $t_n^* = \bar{t}_n / \min \Delta_n$, with $\Delta_n = \bar{t}_n - \bar{t}_{n-1}$ and $n = 2, \ldots, N$. The procedure we use for fitting our models on this data set is as follows. First, we fit a harmonic model to the light curves such that,

$$y_{t_j^*} = \beta_0 + \sum_{i=1}^{p} (\alpha_{1i} \sin(2\pi f i t_j^*) + \beta_{1i} \cos(2\pi f i t_j^*)) + \epsilon_{t_j^*} \quad (4)$$

where $y_{t_j^*}$ is the brightness magnitude of a periodic variable star measured at time t_j^*, with $j = 1, \ldots, n$. In addition, f is the dominant frequency of the light curve estimated by the generalized Lomb–Scargle periodogram (Zechmeister & Kürster 2009). Following Debosscher et al. (2007), we use $p = 4$ harmonics components.

The iARMA model was implemented on the residuals of the harmonic model. From the p-value of the Wald test of both parameters of the iARMA model (pv_ϕ and pv_θ), it is possible to carry out a model selection between the iAR, iMA and iARMA models according to the flowchart presented in Fig. 2. If the p-values of the parameters satisfy $pv_\phi < \alpha$ & $pv_\theta < \alpha$ then the most suitable model is the iARMA. The most suitable model is the iAR if the p-values satisfy $pv_\phi < \alpha$ & $pv_\theta > \alpha$, and the most suitable model is the iMA if the p-values satisfy $pv_\phi > \alpha$ & $pv_\theta < \alpha$. If $pv_\phi > \alpha$ & $pv_\theta > \alpha$ the iARMA model does not have time dependency.

There are three reasons that can explain why on some occasions none of the iARMA model parameters is significant. One is that the fitted data have negative autocorrelation. To verify this, we first use the iMA model to find a negative autocorrelation structure. Consequently, if the parameter θ estimated by the iMA model is less than zero and have a $pv_\theta < \alpha$ we said that the IMA with a negative autocorrelation is a suitable model. If otherwise the IMA model parameter is not significant, we check if the CiAR model finds a negative correlation structure. In that case, the sequence is said to have an autoregressive structure.

Table 6. Model selection with the iARMA Model in the periodic variable stars light curves from OGLE and HIPPARCOS.

Autocorrelation	Positive		Negative		Total	
Model	N	%	N	%	N	%
iAR/CiAR	273	23	181	15	454	39
iMA	32	3	203	17	235	20
iARMA	18	2			18	2
White noise					417	36
Other					47	4
Total	323	28	384	33	1171	100

The second reason for the iARMA model to have parameters that are not significant is that the modelled data have no time dependence. In this case, we say that the sequence is white noise. The Box–Ljung test is used to determine whether the examples, for which the iARMA model finds no temporal dependence, are white noise. If the p-value of the Box–Ljung test is greater than α we says the sequence is white noise. Finally, the third reason is that the iARMA model does not make an adequate fit for the harmonic model residuals. In this application, we define the significance level α as 0.05.

Table 6 shows the model selected for each light curve observed in this data set. As can be seen, the iARMA model was appropriate in 96 per cent of the fitted examples (1124 of 1171 examples). Note that in 36 per cent of the examples analyzed the residuals of the harmonic model have a white noise behaviour. In other words, in these cases the harmonic model explains the dependence structure of the light curve. In addition, in the 28 per cent, we find a positive autocorrelation structure and in 33 per cent we find a negative autocorrelation structure. Among the time-series with positive autocorrelation, the iAR model was adequate in most cases ($N = 273$), followed by the iMA model ($N = 32$) and the iARMA model ($N = 18$). In the time-series with negative autocorrelation, the iMA model was suitable in more than half of the cases ($N = 203$), while the CiAR model was appropriate in 181 cases.

The residuals of a good model show no structure neither in the trend nor in time dependency. In the examples that we fit with the harmonic model, 36 per cent satisfied this condition. The remaining 64 per cent of the residuals that we analyzed had no trend but temporal structure. This result is relevant because it show that in many cases the harmonic model is not sufficient to explain the whole time dependency of the light curve of periodic variable stars.

Figs 3 illustrates an example of the iARMA fit of a light curve observed in the OGLE survey. In this example, we fit the residuals of a semidetatched (or β Lyrae-Type) eclipsing binarie (EB) light curve. This time-series has 332 observations taken over a range of 1226 d. The model selected for this time-series was an iARMA model. The parameter estimated for this model were $\hat{\phi} = 0.80$, $\hat{\theta} = 0.59$ with a variance estimated as $\hat{\sigma^2} = 0.16$. The qq-plot shows a deviation from Gaussianity in the tails of the residuals of the iARMA fit. To verify whether these residuals follow a Gaussian distribution we use the Kolmogorov–Smirnov (KS) test. With a p-value < 0.05 the Gaussianity of the errors is rejected. However, the KS test is not rejected if we compare with a Student's t-distribution with three degrees of freedom (p-value $= 0.24$). In Section 4.5, we show that the QML estimator is robust to Student's t-distributed errors. In addition, the Box–Ljung test shows that the residuals of this fit have no significant autocorrelation at the first 20 lags. Noticed that there is no general rule for selecting the number of lags to be considered

Downloaded from https://academic.oup.com/rasti/article/2/1/33/6987645 by guest on 22 January 2023

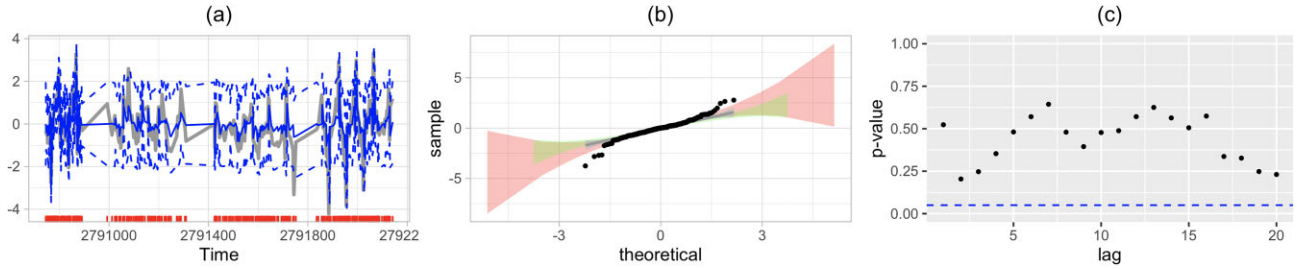


Figure 3. iARMA fit of an irregularly observed time-series. This time-series corresponds to the residuals of an harmonic fit of a semidetatched EB light curve observed in the OGLE survey. Panel (a) shows the time-series fitted by an iARMA model. The grey line is the time-series of the residuals of the harmonic fit, the blue line are the fitted values by the iARMA model, and the dotted blue lines are the upper and lower limits of the confidence interval of each fitted value. Panel (b) shows the qq-plot of the residuals of the iARMA model. In these figures, the grey, green, and red confidence bands correspond to the standard normal distribution, Student's t distribution with 7 degrees of freedom and Student's t distribution with 3 degrees of freedom, respectively. Panel (c) shows the p-value of the Box–Ljung test applied on the residuals of the iARMA model for the 20 first lags.

in the test. Box et al. (2015) suggest the use of at least 20 lags. Selecting too large a number of lags can generate some problems, the most relevant being the quality of the estimates of the ACF, and therefore is not recommended.

Moreover, the performance of the model selected in this example was compared with the state-of-the-art models commonly used to fit light curves. For this purpose, we fit this light curve with the regular ARMA (p, q), CAR (1), and CARMA (2,1) models. In order to implement the ARMA(p, q) model the function *auto.arima* of the *forecast* package in *R* was used. This function determines the order p, q of the ARMA model that obtains the best fit according to the AIC criterion. On the other hand, the models CAR (1) and CARMA (2,1) were implemented using the function *carma* of the *growth* package in *R*. As can be seen in Table E1, the iARMA model (AIC=357.78) obtains a better fit according to the AIC criterion, while the CARMA (2,1) model obtained an AIC of 360.05.

5.2 iARMA implementation on light curves from ZTF

We further implemented the models on light curves of stochastic astronomical objects observed from the ZTF survey in the optical filter g. The ZTF data were obtained through the ALeRCE broker (Förster et al. 2021). Following the classification of astronomical objects of ALeRCE presented by Förster et al. (2021), the stochastic objects considered in this work are Active galactic nuclei, quasi-stellar object (QSO), Blazar, Young-stellar objects and nova/cataclysmic variable star (CV-Nova). On this data set, the iARMA model was implemented on 474 light curves. Before fitting these light curves, their trend was removed with a locally estimated scatter plot smoothing method. This method was implemented using the *sklearn* package of Python. In addition, the observational times were rescaled to ensure that the time gaps between observations are larger than one, as described in the previous section. Model selection on the detrended light curves was implemented following the procedure described in Fig. 2. As in the OGLE and HIPPARCOS example, we use a significance level ofx $\alpha = 0.05$.

In the stochastic objects from ZTF the iARMA model was appropriate in 441 of 474 cases (93.0 per cent). This result is similar to that observed in the OGLE and HIPPARCOS data set. Table 7 shows the frequency with which each model was selected. Note that, in this data set, positive autocorrelation structure is found in 55 per cent of the examples and only in 19 per cent it is found negative autocorrelation. Furthermore, in the remaining 19 per cent of the light curves fitted significant correlation structure was not found. The most commonly selected model in the examples with positive autocorrelation was the iAR model with $N = 222$ examples. The iMA and the iARMA model were selected in 17 and 20 cases, respectively. Among the examples where a negative autocorrelation was found, the most chosen model was the CiAR model ($N = 65$), while the iMA model was chosen in $N = 25$ cases.

Table 7. Model Selection with the iARMA Model in the stochastic objects light curves from ZTF survey.

Autocorrelation	Positive		Negative		Total	
Model	N	%	N	%	N	%
iAR/CiAR	222	47	65	14	287	61
iMA	17	4	25	5	42	9
iARMA	20	4			20	4
White noise					92	19
Other					33	7
Total	259	55	90	19	474	100

Fig. 4 shows the fit of the iARMA family of models on light curves of three stochastic objects from ZTF. The first example is shown in Figs 4(a)–(c), it corresponds to the light curve of a QSO. The time-series has 56 observations taken over a range of ∼388 d. The model selected for this time-series was an iMA model. The parameter estimated by ML for the iMA model was $\hat{\theta} = 0.83$. The variance estimated of the model was $\hat{\sigma^2} = 0.56$. As in the first example, the residuals from this fit are not consistent with a normal distribution. According to the KS test, the residuals follow a Student's t distribution with 3 degrees of freedom (p-value of 0.33). However, as shown in Section 4.5, the QML estimator works well for Student's t distributed errors. The Box–Ljung test was used to verify that the residuals of the iAR model have no significant autocorrelation.

A second example illustrated in Figs 4(d)–(f), shows the light curve of a Blazar. This time-series has 78 observations taken over a range of 522 d. In this case, the model selected was an iARMA model. The parameters estimated by ML were $\hat{\phi} = 0.98$, $\hat{\theta} = 0.56$ with a variance estimated for this model as $\hat{\sigma^2} = 0.22$. Note in Fig. 4(e) that the residuals are Gaussian. Also, the residuals of the fit of the iARMA model have no significant autocorrelation according to the Box–Ljung test.

The third example is another Blazar light curve in which the model selected was an iAR model. The light curve of this Blazar is shown in Fig. 4(g). This time-series has 105 observations taken over a range of 550 d. The parameter estimated by ML was $\hat{\phi} = 0.83$. The variance of the model estimated was $\hat{\sigma^2} = 0.36$. As in the previous example, the residuals of the iAR model are normally distributed.

Downloaded from https://academic.oup.com/rasti/article/2/1/33/6987645 by guest on 22 January 2023

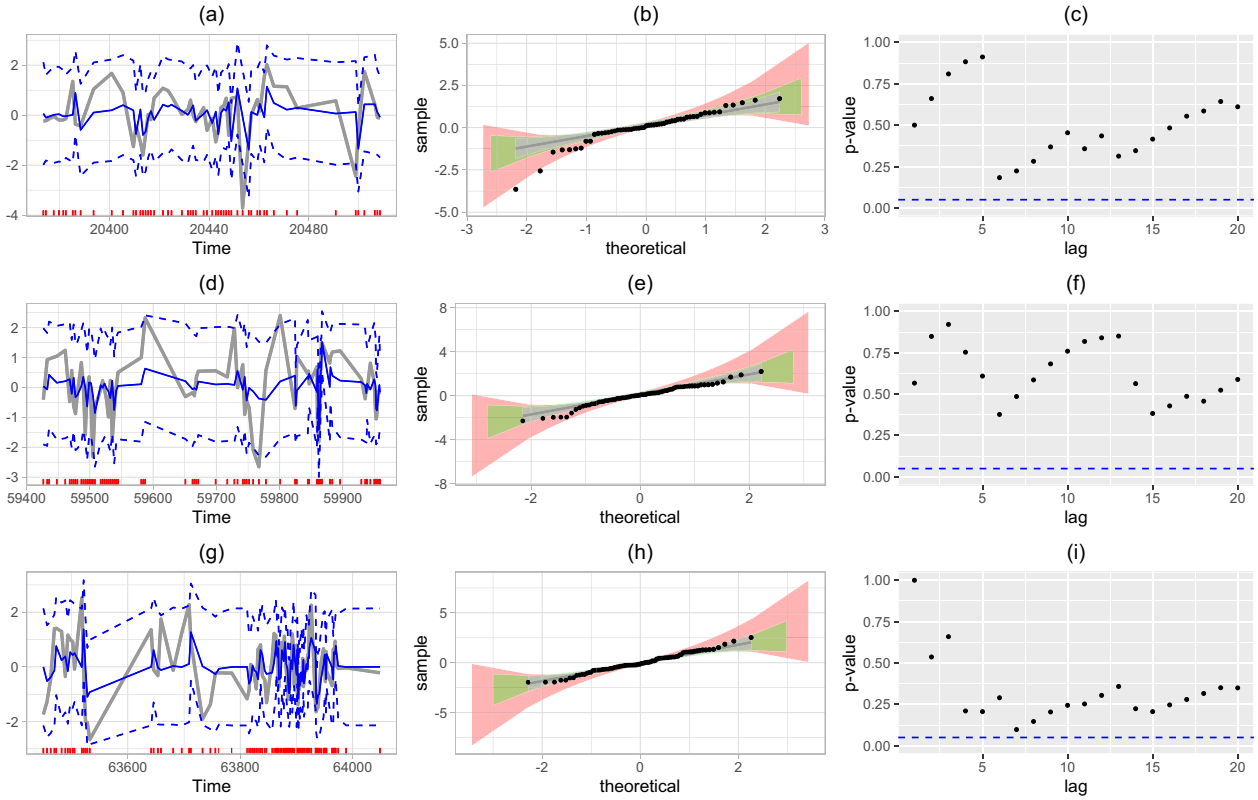


Figure 4. iARMA fit on three examples of detrended light curves of stochastic objects observed in the ZTF Survey. The first row shows the fit on a light curve of a QSO. The second and the third row shows the fit on a light curve of a Blazar. Panels (a)–(g) shows the fitted values. In these figures, the grey line is the time-series of the residuals of the harmonic fit, the blue line are the fitted values by the iARMA model, and the dotted blue lines are the upper and lower limits of the confidence interval of each fitted value. Panels (b)–(h) shows the qq-plot of the residuals of each fit. In these figures, the grey, green, and red confidence bands corresponds to the standard normal distribution, Student's t distribution with 7 degrees of freedom and Student's t distribution with 3 degrees of freedom, respectively. Panels (c)–(i) show the p-values of the Box–Ljung test at the first 20 lags applied on the residuals of each fit.

Furthermore, the residuals also have no significant autocorrelation according to the Box–Ljung test at the first 20 lags as can be seen in Fig. 4(i).

As in the OGLE/HIPPARCOS example, we compare the goodness of fit obtained with the selected models with respect to the ARMA (p, q), CAR (1), and CARMA (2,1) models for the three light curves presented as example in the ZTF data set. Table E1 shows that for the three examples, the iARMA methodology obtained a lower AIC than the other models evaluated, obtaining the best fit to these data. Particularly, for the QSO light curve, the AIC obtained with the selected iMA model was 76.28, while the CAR(1) model obtained an AIC of 78.09. For the Blazar light curve presented in the second example, the AIC obtained with the selected iARMA model was 100.29, lower than the obtained with the CAR(1) model (AIC=103.30). Finally, for the last example, the lowest AIC is reached with the iAR model (AIC=129.79), followed by the CAR(1) model (AIC=130.78).

6 CONCLUSIONS

This paper proposes an irregularly spaced model that allows for the handling of first-order MA structures with irregularly spaced times. It formal definition is provided and some of its statistical properties are studied. State space representations, along with one-step linear predictors, are also provided. Furthermore, the finite-sample performance of the proposed estimation methods is studied by means of Monte Carlo simulations for both Gaussian and non-Gaussian distribution errors. The proposed methods display good estimation performance.

The proposed model was applied on two data sets with light curves of astronomical objects. We show that the iMA model was the most suitable fit in 20 per cent of the OGLE/HIPPARCOS examples and in 9 per cent of the ZTF examples. In addition, we found that in 33 per cent of the OGLE/HIPPARCOS examples a negative autocorrelation was estimated. In more than half of these cases, the most appropriate model was the iMA. For light curves from ZTF stochastic object, the proportion of examples estimated with negative correlation was lower (19 per cent). In about 30 per cent (25 of 90) of these cases, the iMA model fully explained the serial correlation of the light curve.

We illustrate the fit of the iARMA models in four light curves from OGLE/HIPPARCOS and ZTF. In two of these light curves, the qq-plot of the residuals shows a consistent behaviour with Gaussian errors, while in the other two light curves the qq-plot show deviation from Gaussianity and more consistent with a Student's t distribution for the errors. However, in Section 4.5, it is shown that the QML estimators are not affected with these deviations from Gaussianty. In addition, the iARMA methodology exhibits better goodness of fit performance as compared to the alternative models, such as the ARMA (p, q), CAR (1) and CARMA (2,1).

These results show that the iMA model offers a useful alternative to iAR processes for light curve fitting. Particularly, for the case, where the serial dependence of the light curve is negative. This is

Downloaded from https://academic.oup.com/rasti/article/2/1/33/6987645 by guest on 22 January 2023

because the iMA model has a time dependence structure that differs from that offered by an autoregressive model such as the CiAR. While autoregressive models have an autocorrelation structure of exponential decay, MA models are only correlated with respect to the nearest observation.

In addition, it is important to emphasize that the proposed model is not similar to any processes generally used to model irregularly observed data. For example, the CARMA (p, q) models are defined only for $p > q$. In other words, the MA part of the CARMA process only exists if the process has a higher order autoregressive structure. In addition, the iMA model is also not equivalent to a regular MA model with missing observations, since in this kind of process, a missing observation generates two independent blocks of observations.

With this work, we are contributing with a novel method to the state-of-the-art models used to explain the time dependence of light curves on irregularly observed sequences.

The code to implement the iMA model is available in R upon request to the authors.

ACKNOWLEDGEMENTS

OC was supported by CONICYT PFCHA/2015-21151457. PW, ES, and EF were supported by the ANID Millennium Science Initiative ICN12_009, awarded to the Millennium Institute of Astrophysics. EF was supported by ANID grant Fondecyt Iniciacion 11200590.

DATA AVAILABILITY

The OGLE/HIPPARCOS light curves data set is available in https://github.com/felipeelorrieta/Datasets. The ZTF light curves data set is available from the ALeRCE website: http://alerce.science/.

REFERENCES

Adorf H. M., 1995, in Shaw R. A., Payne H. E., Hayes J. J. E., eds, ASP Conf. Ser. Vol. 77, Astronomical Data Analysis Software and Systems IV. Astron. Soc. Pac., San Francisco, p. 460
Babu G. J., Mahabal A., 2016, Int. Stat. Rev., 84, 506
Belcher J., Hampton J. S., Tunnicliffe Wilson G., 1994, J. R. Stat. Soc. B, 56, 141
Bellm E. C. et al., 2018, Publ. Astron. Soc. Pac., 131, 018002
Bose A., 1990, Ann. Inst. Stat. Math, 42, 753
Box G. E. P., Jenkins G. M., Reinsel G. C., Ljung G. M., 2015, Time-series Analysis: Forecasting and Control, 5th edn. John Wiley & Sons, Inc. Hoboken, New Jersey
Brockwell P. J., Davis R. A., 1991, Time-series: Theory and Methods, 2nd edn. Springer Series in Statistics. Springer Science + Business Media, LLC, New York, NY
Byrd R. H., Lu P., Nocedal J., Zhu C., 1995, SIAM J. Sci. Comput., 16, 1190
Caceres G. A., Feigelson E. D., Babu G. J., Bahamonde N., Christen A., Bertin K., Meza C., Curé M., 2019, AJ, 158, 57
Corduas M., Piccolo D., 2008, Comput. Stat. Data Anal., 52, 1860
Debosscher J., Sarro L. M., Aerts C., Cuypers J., Vandenbussche B., Garrido R., Solano E., 2007, A&A, 475, 1159
Dunsmuir W., 1983, Stoch. Process. Appl., 14, 279
Edelmann D., Fokianos K., Pitsillou M., 2019, Int. Stat. Rev., 87, 237
Elorrieta F., Eyheramendy S., Palma W., 2019, A&A, 627, A120
Elorrieta F., Eyheramendy S., Palma W., Ojeda C., 2021, MNRAS, 505, 1105
Eyheramendy S., Elorrieta F., Palma W., 2018, MNRAS, 481, 4311
Förster F. et al., 2021, AJ, 161, 242
Ghalanos A., 2020, rugarch: Univariate GARCH models, R package version 1.4-4
Hamilton J. D., 1994, Time-series Analysis. Princeton Univ. Press, Princeton, NJ
Hand D. J., 2008, Int. Stat. Rev., 76, 458
Harvey A. C., 1989, Forecasting, Structural Time-series Models and the Kalman filter. Cambridge Univ. Press, Cambridge
Harvill J. L., Ravishanker N., Ray B. K., 2013, Comput. Stat. Data Anal., 64, 113
Kim J., Stoffer D. S., 2008, J. Time Ser. Anal., 29, 811
Koehler E., Brown E., Haneuse S. J., 2009, Am. Stat., 63, 155
Miller J. I., 2019, J. Time Ser. Anal., 40, 936
Moore M. I., Visser A. W., Shirtcliffe T., 1987, J. Time Ser. Anal., 8, 433
Mudelsee M., 2014, Climate Time-Series Analysis: Classical Statistical and Bootstrap Methods, Atmospheric and Oceanographic Sciences Library, Vol. 51, 2nd edn. Springer International Publishing, Heidelberg, New York, Dordrecht, London
Muñoz A., Carey V., Schouten J. P., Segal M., Rosner B., 1992, Biometrics, 48, 733
Ojeda C., Palma W., Eyheramendy S., Elorrieta F., 2022, Selected Contributions from ITISE 2021, Contributions to Statistics. Springer, Cham, Gran Canaria
Parzen E., 1963, Indian J. Stat. A , 25, 383
Parzen E., ed., 1984, Time-series Analysis of Irregularly Observed Data, Lecture Notes in Statistics, Vol. 25, Feb. 10–13, 1983. Springer-Verlag, College Station, TX
Perryman M. A. C. et al., 1997, A&A, 323, L49
Phadke M. S., Wu S. M., 1974, J. Am. Stat. Assoc., 69, 325
Podgorski K., 2014, Int. Stat. Rev., 82, 153
Reinsel G. C., Wincek M. A., 1987, Biometrika, 74, 115
Robinson P. M., 1977, Stoch. Process. Appl., 6, 9
Shumway R. H., Stoffer D. S., 2017, Time-series Analysis and its Applications with R examples, 4th edn., Springer Texts in Statistics. Springer International Publishing, Cham
Spanos A., 1999, Probability Theory and Statistical Inference: Econometric Modeling with Observational Data. Cambridge Univ. Press, Cambridge
Stout W. F., 1974, Almost Sure Convergence, Probability and Mathematical Statistics No. 24. Academic Press, Inc., New York, San Francisco, London
Thornton M. A., Chambers M. J., 2013, J. Time Ser. Anal., 34, 552
Udalski A., Soszynski I., Szymanski M., Kubiak M., Pietrzynski G., Wozniak P., Zebrun K., 1999, Acta Astron, 49, 223
Zechmeister M., Kürster M., 2009, A&A, 496, 577
Zhang S., 2020, Comput. Stat. Data Anal., 151, 107019

APPENDIX A: BOOTSTRAP

Following Bose (1990), for $n \geq 2$, define the estimated innovations or one-step prediction residuals, as

$$e_{t_n} = X_{t_n} + \sum_{j=1}^{n-1} (-1)^j \frac{\prod_{k=n-j+1}^{n} \theta^{\Delta_k}}{\prod_{l=n-j}^{n-1} c_l(\theta)} X_{t_{n-j}}$$

and $e_{t_1} = X_{t_1}$. Using the structure of the process and assuming that the fitted model is, in fact, the true model for the data, the residuals are given by

$$e_{t_n} = \varepsilon_{t_n} + (-1)^{n-2} \frac{\prod_{k=2}^{n} \theta^{\Delta_k}}{\prod_{l=1}^{n-1} c_l(\theta)} \varepsilon_{t_1}.$$

Hence, e_{t_n} and ε_{t_n} are close for all large n if $0 \leq \theta < 1$, which shows that resampling is proper in this situation.

APPENDIX B: MEASURES OF PERFORMANCE REGULARLY SPACED CASE

In this section, the performance of irregularly spaced case for the ML and Bootstrap estimators is compared in the context of regularly spaced times. Tables B1 and B2 show the Monte Carlo results.

Downloaded from https://academic.oup.com/rasti/article/2/1/33/6987645 by guest on 22 January 2023

Table B1. Monte Carlo results for the ML estimator with regularly spaced times. The maximum MCE estimated (across scenarios) is 0.0004.

N	θ	$\hat{\theta}^{\text{MLE}}$	$\widehat{\text{se}}(\hat{\theta}^{\text{MLE}})$	$\widetilde{\text{se}}(\hat{\theta}^{\text{MLE}})$	$\text{se}(\hat{\theta}^{\text{MLE}})$	$\text{bias}_{\hat{\theta}^{\text{MLE}}}$	$\text{RMSE}_{\hat{\theta}^{\text{MLE}}}$	$\text{CV}_{\hat{\theta}^{\text{MLE}}}$
300	−0.90	−0.91	0.03	0.03	0.025	−0.01	0.03	0.03
	−0.70	−0.71	0.04	0.04	0.041	−0.01	0.04	0.06
	−0.50	−0.51	0.05	0.05	0.050	−0.01	0.05	0.10
	0.50	0.50	0.05	0.05	0.050	0.00	0.05	0.10
	0.70	0.70	0.04	0.04	0.041	0.00	0.04	0.06
	0.90	0.90	0.03	0.03	0.025	0.00	0.03	0.03
1000	−0.90	−0.90	0.01	0.01	0.014	−0.00	0.01	0.02
	−0.70	−0.70	0.02	0.02	0.023	−0.00	0.02	0.03
	−0.50	−0.50	0.03	0.03	0.027	−0.00	0.03	0.05
	0.50	0.50	0.03	0.03	0.027	−0.00	0.03	0.06
	0.70	0.70	0.02	0.02	0.023	−0.00	0.02	0.03
	0.90	0.90	0.01	0.01	0.014	0.00	0.01	0.02

Table B2. Monte Carlo results for the bootstrap estimator with regularly spaced times. The maximum MCE estimated (across scenarios) is 0.0004.

N	θ	$\hat{\theta}^{\text{b}}$	$\widehat{\text{se}}(\hat{\theta}^{\text{b}})$	$\widetilde{\text{se}}(\hat{\theta}^{\text{b}})$	$\text{bias}_{\hat{\theta}^{\text{b}}}$	$\text{RMSE}_{\hat{\theta}^{\text{b}}}$	$\text{CV}_{\hat{\theta}^{\text{b}}}$
300	−0.90	−0.91	0.03	0.02	−0.01	0.03	0.03
	−0.70	−0.72	0.04	0.04	−0.02	0.05	0.06
	−0.50	−0.51	0.05	0.05	−0.01	0.05	0.10
	0.50	0.50	0.05	0.05	0.00	0.05	0.10
	0.70	0.70	0.04	0.04	0.00	0.04	0.06
	0.90	0.91	0.03	0.03	0.01	0.03	0.03
1000	−0.90	−0.91	0.01	0.01	−0.01	0.02	0.02
	−0.70	−0.71	0.02	0.02	−0.01	0.02	0.03
	−0.50	−0.51	0.03	0.03	−0.01	0.03	0.05
	0.50	0.50	0.03	0.03	−0.00	0.03	0.06
	0.70	0.70	0.02	0.02	0.00	0.02	0.03
	0.90	0.90	0.01	0.01	0.00	0.01	0.02

In addition, Table B1, also consider the asymptotic standard error for the ML estimator defined as the square root of

$$\text{se}^2(\hat{\theta}^{\text{MLE}}) = \frac{1-\theta^2}{N}. \tag{B1}$$

From these tables, notice that the Monte Carlo results for the regularly spaced time case exhibit a similar behaviour as compared to the irregularly spaced time case.

APPENDIX C: MEASURES OF PERFORMANCE IN COMPARISON WITH CARMA (2,1) MODEL

In Tables C1 and C2, it is presented other goodness of fit measures such as the Akaike Criterion and the –2 log-likelihood to compare the performance of the iMA and CARMA (2,1) models in fitting iMA model.

Table C1. Monte Carlo results of the experiment to compare the performance of the iMA and CARMA (2,1) models in fitting iMA model. The goodness of fit measure estimated from both models is the –2 Log-likelihood.

N	θ	$\hat{\theta}$	$\widehat{\text{se}}(\hat{\theta})$	−2LL_iMA	SD(−2LL_iMA)	−2LL_C21	SD(−2LL_C21)	% success
300	−0.9	−0.9029	0.0270	926.0067	24.4143	1002.6260	37.8083	100.00
	−0.7	−0.7048	0.0569	919.4303	24.3060	960.3786	28.6553	99.10
	−0.5	−0.5029	0.0715	894.4120	24.2160	908.0760	25.8383	93.40
	0.5	0.4910	0.0715	894.3942	24.3517	895.6509	25.3111	52.30
	0.7	0.6932	0.0576	919.3802	24.3470	923.5709	25.4748	75.40
	0.9	0.8973	0.0283	925.9526	24.2864	955.2145	27.0834	99.60
1000	−0.9	−0.9009	0.0149	3088.3858	44.1965	3392.1862	81.6827	100.00
	−0.7	−0.7018	0.0311	3067.1376	44.1096	3219.6285	54.5811	100.00
	−0.5	−0.5019	0.0387	2983.8971	44.0633	3043.5553	47.3148	99.40
	0.5	0.4974	0.0387	2983.8594	44.1790	2996.9374	47.7540	72.30
	0.7	0.6981	0.0312	3067.0158	44.1788	3087.4784	45.2897	98.80
	0.9	0.8992	0.0151	3088.2274	44.1532	3193.1205	47.9557	100.00

Table C2. Monte Carlo results of the experiment to compare the performance of the iMA and CARMA (2,1) models in fitting iMA model. The goodness of fit measure estimated from both models is the AIC.

N	θ	$\hat{\theta}$	$\widehat{\text{se}}(\hat{\theta})$	AIC_iMA	SD(AIC_iMA)	AIC_C21	SD(AIC_C21)	% success
300	−0.9	−0.9029	0.0270	928.0067	24.4143	1004.6260	37.8083	100.00
	−0.7	−0.7048	0.0569	921.4303	24.3060	962.3786	28.6553	99.10
	−0.5	−0.5029	0.0715	896.4120	24.2160	910.0760	25.8383	93.40
	0.5	0.4910	0.0715	896.3942	24.3517	897.6509	25.3111	52.30
	0.7	0.6932	0.0576	921.3802	24.3470	925.5709	25.4748	75.40
	0.9	0.8973	0.0283	927.9526	24.2864	957.2145	27.0834	99.60
1000	−0.9	−0.9009	0.0149	3090.3858	44.1965	3394.1862	81.6827	100.00
	−0.7	−0.7018	0.0311	3069.1376	44.1096	3221.6285	54.5811	100.00
	−0.5	−0.5019	0.0387	2985.8971	44.0633	3045.5553	47.3148	99.40
	0.5	0.4974	0.0387	2985.8594	44.1790	2998.9374	47.7540	72.30
	0.7	0.6981	0.0312	3069.0158	44.1788	3089.4784	45.2897	98.80
	0.9	0.8992	0.0151	3090.2274	44.1532	3195.1205	47.9557	100.00

APPENDIX D: MEASURES OF PERFORMANCE FOR BOOTSTRAP ESTIMATOR-NON GAUSSIAN CASE

Below has presented in Tables D1 and D2 the performance of the Bootstrap estimator when non-Gaussian errors are assumed.

Table D1. Monte Carlo results for the bootstrap estimator with irregularly spaced times and Student's t errors with shape parameter $\nu = 7$. The maximum MCE estimated (across scenarios) is 0.0005.

N	θ	$\hat{\theta}^{\text{b}}$	$\widehat{\text{se}}(\hat{\theta}^{\text{b}})$	$\widetilde{\text{se}}(\hat{\theta}^{\text{b}})$	$\text{bias}_{\hat{\theta}^{\text{b}}}$	$\text{RMSE}_{\hat{\theta}^{\text{b}}}$	$\text{CV}_{\hat{\theta}^{\text{b}}}$
300	−0.90	−0.91	0.03	0.03	−0.01	0.03	0.03
	−0.70	−0.70	0.06	0.07	0.00	0.06	0.09
	−0.50	−0.49	0.08	0.09	0.01	0.08	0.15
	0.50	0.48	0.08	0.09	−0.02	0.08	0.16
	0.70	0.69	0.06	0.07	−0.01	0.06	0.09
	0.90	0.90	0.03	0.03	−0.00	0.03	0.03
1000	−0.9	−0.90	0.01	0.02	−0.00	0.01	0.02
	−0.70	−0.70	0.03	0.04	0.00	0.03	0.05
	−0.50	−0.50	0.04	0.05	0.00	0.04	0.08
	0.50	0.49	0.04	0.05	−0.01	0.04	0.08
	0.70	0.69	0.03	0.04	−0.01	0.03	0.05
	0.90	0.90	0.02	0.02	−0.00	0.02	0.02

Table D2. Monte Carlo results for the bootstrap estimator with irregularly spaced times and generalized errors with shape parameter $\kappa = 1.28$. The maximum MCE estimated (across scenarios) is 0.0005.

N	θ	$\hat{\theta}^{\text{b}}$	$\widehat{\text{se}}(\hat{\theta}^{\text{b}})$	$\widetilde{\text{se}}(\hat{\theta}^{\text{b}})$	$\text{bias}_{\hat{\theta}^{\text{b}}}$	$\text{RMSE}_{\hat{\theta}^{\text{b}}}$	$\text{CV}_{\hat{\theta}^{\text{b}}}$
300	−0.90	−0.90	0.03	0.03	−0.00	0.03	0.03
	−0.70	−0.70	0.06	0.07	0.00	0.06	0.09
	−0.50	−0.49	0.08	0.09	0.01	0.08	0.15
	0.50	0.48	0.08	0.09	−0.02	0.08	0.16
	0.70	0.68	0.06	0.07	−0.02	0.06	0.09
	0.90	0.90	0.03	0.03	−0.00	0.03	0.03
1000	−0.90	−0.90	0.02	0.02	−0.00	0.02	0.02
	−0.70	−0.70	0.03	0.04	0.00	0.03	0.05
	−0.50	−0.50	0.04	0.05	0.00	0.04	0.08
	0.50	0.49	0.04	0.05	−0.01	0.04	0.08
	0.70	0.70	0.03	0.03	−0.00	0.03	0.05
	0.90	0.90	0.02	0.02	−0.00	0.02	0.02

Downloaded from https://academic.oup.com/rasti/article/2/1/33/6987645 by guest on 22 January 2023

APPENDIX E: COMPARISON WITH THE STATE OF THE ART OF TIME-SERIES MODELS IN LIGHT CURVES EXAMPLES

Below, we present in Table E1 a comparison of the iARMA models with the state-of-the-art models commonly used to fit light curves for the four examples that were presented in Section 5.

Table E1. AIC obtained in the four light curves examples presented in this work for the state-of-the-art time-series models used for irregularly observed data.The example EB-OH corresponds to the Fig. 3(a), while the examples QSO-ZTF, Blazar1-ZTF, and Blazar2-ZTF correspond to the Figs 4(a)–(g), respectively.

Model	EB-OH	QSO-ZTF	Blazar1-ZTF	Blazar2-ZTF
iARMA	**357.78**	**76.28**	**100.29**	**129.79**
ARMA (p, q)	773.77	155.83	208.67	280.25
CAR (1)	366.08	78.09	103.30	130.78
CARMA (2,1)	360.05	79.44	103.31	139.08

This paper has been typeset from a TEX/LATEX file prepared by the author.

Downloaded from https://academic.oup.com/rasti/article/2/1/33/6987645 by guest on 22 January 2023